

Proposal to Search for Heavy Neutral Leptons at the SPS

W. Bonivento^{1,2}, A. Boyarsky³, H. Dijkstra², U. Egede⁴, M. Ferro-Luzzi², B. Goddard², A. Golutvin⁴,
D. Gorbunov⁵, R. Jacobsson², J. Panman², M. Patel⁴, O. Ruchayskiy⁶, T. Ruf², N. Serra⁷, M. Shaposhnikov⁶,
D. Treille² (†)

¹*Sezione INFN di Cagliari, Cagliari, Italy*

²*European Organization for Nuclear Research (CERN), Geneva, Switzerland*

³*Instituut-Lorentz for Theoretical Physics, Universiteit Leiden, Niels Bohrweg 2, Leiden, The Netherlands*

⁴*Imperial College London, London, United Kingdom*

⁵*Institute for Nuclear Research of the Russian Academy of Sciences (INR RAN), Moscow, Russia*

⁶*Ecole Polytechnique Fédérale de Lausanne (EPFL), Lausanne, Switzerland*

⁷*Physik-Institut, Universität Zürich, Zürich, Switzerland*

(†) *retired*

Executive Summary

A new fixed-target experiment at the CERN SPS accelerator is proposed that will use decays of charm mesons to search for Heavy Neutral Leptons (HNLs), which are right-handed partners of the Standard Model neutrinos. The existence of such particles is strongly motivated by theory, as they can simultaneously explain the baryon asymmetry of the Universe, account for the pattern of neutrino masses and oscillations and provide a Dark Matter candidate.

Cosmological constraints on the properties of HNLs now indicate that the majority of the interesting parameter space for such particles was beyond the reach of the previous searches at the PS191, BEBC, CHARM, CCFR and NuTeV experiments. For HNLs with mass below 2 GeV, the proposed experiment will improve on the sensitivity of previous searches by four orders of magnitude and will cover a major fraction of the parameter space favoured by theoretical models.

The experiment requires a 400 GeV proton beam from the SPS with a total of 2×10^{20} protons on target, achievable within five years of data taking. The proposed detector will reconstruct exclusive HNL decays and measure the HNL mass. The apparatus is based on existing technologies and consists of a target, a hadron absorber, a muon shield, a decay volume and two magnetic spectrometers, each of which has a 0.5 Tm magnet, a calorimeter and a muon detector. The detector has a total length of about 100 m with a 5 m diameter. The complete experimental set-up could be accommodated in CERN's North Area.

The discovery of a HNL would have a great impact on our understanding of nature and open a new area for future research.

1 Introduction

The new scalar particle with mass $M_H = 125.5 \pm 0.2_{stat} {}^{+0.5}_{-0.6}_{syst}$ GeV (ATLAS) [1], $M_H = 125.7 \pm 0.3_{stat} \pm 0.3_{syst}$ GeV (CMS) [2], recently found at the LHC, has properties consistent with those of the

long-awaited Higgs boson of the Standard Model (SM) [3]. This discovery implies that the Landau pole in the Higgs self-interaction is well above the quantum gravity scale $M_{Pl} \simeq 10^{19}$ GeV (see, e.g. Ref. [4]). Moreover, within the SM, the vacuum is stable, or metastable with a lifetime exceeding that of the Universe by many orders of magnitude [5]. Without the addition of any further new particles, the SM is therefore an entirely self-consistent, weakly-coupled, effective field theory all the way up to the Planck scale (see Refs. [5, 6] for a recent discussion).

Nevertheless, it is clear that the SM is incomplete. Besides a number of fine-tuning problems (such as the hierarchy and strong CP problems), the SM is in conflict with the observations of non-zero neutrino masses, the excess of matter over antimatter in the Universe, and the presence of non-baryonic dark matter.

The most economical theory that can account simultaneously for neutrino masses and oscillations, baryogenesis, and dark matter, is the neutrino minimal Standard Model (ν MSM) [7, 8]. It predicts the existence of three Heavy Neutral Leptons (HNL) and provides a guideline for the required experimental sensitivity [9]. The search for these HNLs is the focus of the present proposal.

In addition to HNLs, the experiment will be sensitive to many other types of physics models that produce weakly interacting exotic particles with a subsequent decay inside the detector volume, see e.g. Refs. [10–15]. Longer lifetimes and smaller couplings would be accessible compared to analogous searches performed previously by the CHARM experiment [16].

In the remainder of this document the theoretical motivation for HNL searches is presented in Section 2 and the limits from previous experimental searches are then detailed in Section 3. The proposed experimental set-up is presented in Section 4 and in Section 5 the background sources are discussed, before the expected sensitivity is calculated in Section 6. The conclusions are presented in Section 7.

2 Theoretical motivation

In type-I seesaw models (for a review see Ref. [17]) the extension of the SM fermion sector by three right-handed (Majorana) leptons, N_I , where $I = (1, 2, 3)$, makes the leptonic sector similar to the quark sector (see Fig. 1). Irrespective of their masses, these neutral leptons can explain the flavour oscillations of the active neutrinos. Four different domains of HNL mass, M_N , are usually considered:

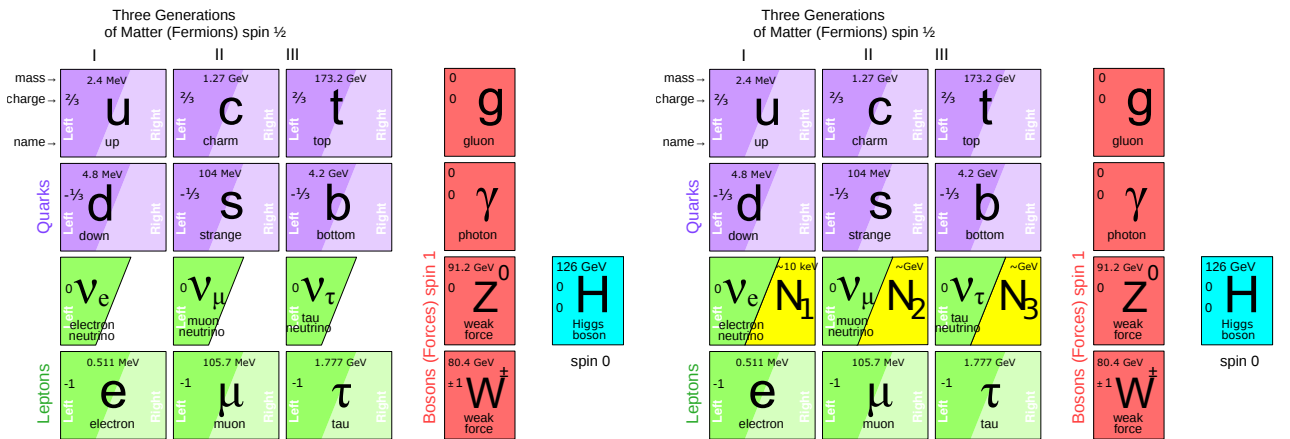


Figure 1: Particle content of the SM and its minimal extension in the neutrino sector. In the (left) SM the right-handed partners of neutrinos are absent. In the (right) ν MSM all fermions have both left- and right-handed components and masses below the Fermi scale.

- (1) Models with HNLs with $10^9 < M_N < 10^{14}$ GeV [18] are motivated by Grand Unified Theories. In such theories the observed baryon asymmetry of the Universe originates in CP-violating decays of the HNLs, which produce a lepton asymmetry [19]. This asymmetry is then converted into a baryon asymmetry by sphalerons [20, 21]. The large mass of the HNLs results in a fine-tuning problem for the Higgs mass. A natural solution is provided by low energy supersymmetry but at present this is not supported by experimental evidence. Theories with very heavy neutral leptons are unable to account for dark matter and cannot be directly probed by experiments;
- (2) Models with $M_N \sim 10^2 - 10^3$ GeV (for a review see Ref. [22]) are motivated by a possible solution to the hierarchy problem at the electroweak scale (see e.g. Ref. [23]). The baryon asymmetry of the Universe can be produced via resonant leptogenesis and sphalerons [24]. As above, there is no candidate for dark matter particles. A portion of the parameter space can be accessed by direct searches at the ATLAS and CMS experiments [25];
- (3) Models with masses of the HNLs below the Fermi scale and roughly of the order of the masses of the known quarks and leptons, are able to account for neutrino masses and oscillations and can also give rise to the baryon asymmetry of the Universe and can provide dark matter [7, 8, 26–28] (for a review see Ref. [29]). The phenomenology of GeV-scale HNLs was previously studied in Refs. [30–33]. Owing to its relatively large mass, the dark matter candidate – the $\mathcal{O}(10)$ keV HNL, does not contribute to the number of relativistic neutrino species measured recently by the Planck satellite [34];
- (4) Models with $M_N \sim \text{eV}$ [35] are motivated by the $2-3\sigma$ deviations observed in short-baseline neutrino-oscillation experiments [36, 37], reactor neutrino experiments [38] and gallium solar neutrino experiments [39–42]. Such neutral leptons are usually referred to as sterile neutrinos. Theories involving these sterile neutrinos can explain neither the baryon asymmetry of the Universe nor dark matter.

The GeV-scale HNLs of category (3) are able to solve all major problems of the SM and the search for such particles is the focus of the present proposal.

2.1 The Neutrino Minimal Standard Model

The most general renormalisable Lagrangian of all SM particles and three singlet (with respect to the SM gauge group) fermions, N_I , is

$$L_{\text{singlet}} = i\bar{N}_I\partial_\mu\gamma^\mu N_I - Y_{I\alpha}\bar{N}_I^c\tilde{H}L_\alpha^c - M_I\bar{N}_I^c N_I + \text{h.c.}, \quad (1)$$

where L_α , $\alpha = e, \mu, \tau$ are the SM lepton doublets, c is the superscript denoting the charge conjugation, $\tilde{H}_i = \epsilon_{ij}H_j^*$, where H is the SM Higgs doublet, and $Y_{I\alpha}$ are the relevant Yukawa couplings. The last term is the Majorana mass term, which is allowed as the N_I carry no gauge charges. When the SM Higgs field gains a non-zero vacuum expectation value, $v = 246$ GeV, the Yukawa term in Eqn. (1) results in mixing between the HNLs and the SM neutrinos. In the mass basis, the massive active-neutrino states mix with each other, as is required to explain neutrino oscillations.

The model given by Eqn. (1) contains eighteen new parameters compared to the SM (six CP-violating phases, six mixing angles, three Dirac masses, and three Majorana masses). Five of these parameters (related to three mixing angles of the active neutrinos and two mass differences) have been determined by low-energy neutrino experiments [43]. The large number of CP-violating phases opens the possibility of significantly larger CP violation than that seen in the quark sector. In particular, the baryon asymmetry of the Universe can be explained by a wide range of parameters [44]. In fact,

HNLs with any mass difference and mixing angle allowed by experimental constraints can produce the necessary baryon asymmetry in the Universe (BAU).

The most interesting variant of this model is the ν MSM. In this model, the lightest singlet fermion, N_1 , has a very weak mixing with the other leptons, playing no role in active-neutrino mass generation. The lightest singlet N_1 is then sufficiently stable to be a dark matter candidate. This particle could be detected by searching for a narrow line in the X-ray spectrum coming from radiative decays $N_1 \rightarrow \nu\gamma$ (for a review see Ref. [29]). The reduced number of parameters that arises from requiring that N_1 be a dark matter candidate results in the further requirement that $N_{2,3}$ be nearly degenerate in mass. This enables CP violation to be enhanced to the level required to explain the baryon asymmetry in the Universe.

The order of magnitude of the different parameters in Eqn. (1) can be understood by considering the typical value of the Dirac mass term, $m_D \sim Y_{I\alpha}v$. The scale of the active neutrino masses is given by the seesaw formula,

$$m_\nu \sim \frac{m_D^2}{M}. \quad (2)$$

For the HNL mass $M \sim 1 \text{ GeV}$, and $m_\nu \sim 0.05 \text{ eV}$, the value of m_D is in the region of 10 keV , and the Yukawa couplings are of the order of 10^{-7} .

Denoting the mixing angles between N_I and active neutrinos of flavour α by $U_{I\alpha} = Y_{I\alpha}v/\sqrt{2}M$, the integral mixing angle,

$$U^2 = \sum_{I,\alpha} |U_{I\alpha}|^2, \quad (3)$$

measures the overall strength of interactions between the N_I and the active neutrinos. At a given mass, M , a larger U yields stronger interactions (mixing) of the singlet fermions and the SM leptons. In the early Universe, large U would result in the $N_{2,3}$ particles coming into equilibrium above the electroweak temperature and would therefore erase any baryon asymmetry in the Universe. A small mixing between the neutral leptons and the active neutrinos would enable HNLs to generate the observed baryon asymmetry of the Universe and would also explain why these particles have not yet been observed in experiments.

2.2 Heavy Neutral Leptons – production and decay mechanisms

In the ν MSM the HNL-neutrino mixing gives rise to HNL ($N_{2,3}$) production in weak decays of heavy mesons. The same mixing gives rise to the decay of the HNLs to SM particles. The allowed mixing angles are small and the $N_{2,3}$ particles are much longer-lived (by a factor $\sim 1/U^2$) than weakly decaying SM particles of similar mass (see Fig. 2). For HNL masses below the charm threshold, the most relevant production mechanisms are shown in Fig. 3 (left). The requirement for mixing into active neutrinos at both production and decay results in signal yields which depend on the fourth power of the HNL-neutrino mixing, U^4 .

Potential two- and three-body decay modes of $N_{2,3}$ are shown in Fig. 3 (right). For D mesons, the typical branching fractions expected for the upper and lower limits of the ν MSM parameter space are at the level of [9]

$$\mathcal{B}_{D \rightarrow N} \sim 10^{-8} - 10^{-12}. \quad (4)$$

The three-body leptonic decay branching fractions depend on the flavour pattern of HNL-to-active neutrino mixing: $\mathcal{B}(N \rightarrow \nu l_1^+ l_2^-) \simeq 1 - 10\%$ ($l_{1,2} = e, \mu$). Among the two-body decays the most promising for searches are¹ $\mathcal{B}(N \rightarrow e^- \pi^+) \simeq 0.2\% - 50\%$, $\mathcal{B}(N \rightarrow \mu^- \pi^+) \simeq 0.1\% - 50\%$, $\mathcal{B}(N \rightarrow e^- \rho^+) \simeq 0.5\% - 20\%$, $\mathcal{B}(N \rightarrow \mu^- \rho^+) \simeq 0.5\% - 20\%$. Branching fractions to $e^- K^+$ and $\mu^- K^+$ are

¹ In the following, charge conjugation is implied unless stated otherwise.

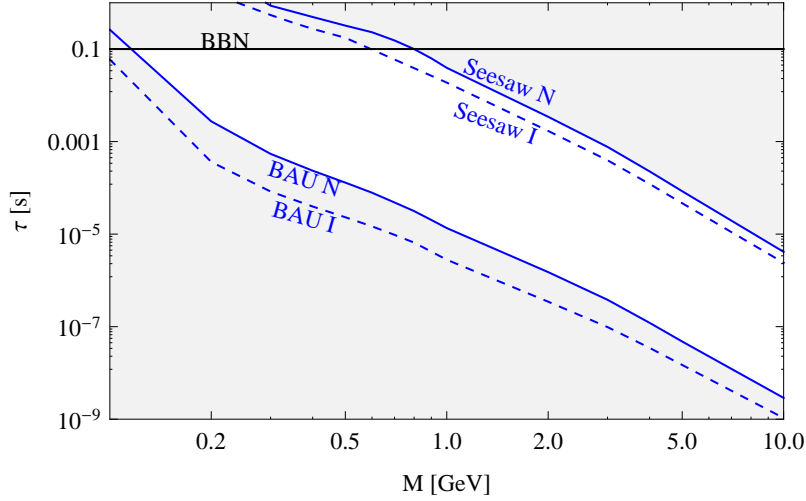


Figure 2: Constraints on the HNL lifetime, τ , from Big Bang Nucleosynthesis (black line: “BBN”), from the baryon asymmetry of the Universe (“BAU”) and from the seesaw mechanism (blue solid lines: “BAU N” and “Seesaw N” refer to a normal mass-hierarchy of active neutrinos and “BAU I” and “Seesaw I” refer to an inverted mass-hierarchy). The allowed region of the parameter space is shown in white for the normal hierarchy case. The limits from direct experimental searches are outlined in Fig. 4. Figure taken from Ref. [45].

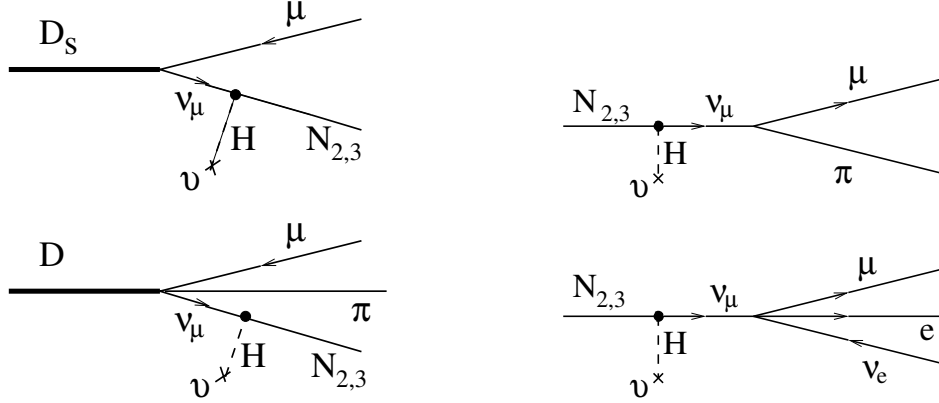


Figure 3: Feynman diagrams (left) for the production of HNLs and (right) for their decays. The dashed line denotes the coupling to the Higgs vacuum expectation value, leading to the mixing of active neutrinos and HNLs via Yukawa couplings.

always below 2%. The $\mu^-\pi^+$ final state is the cleanest signature experimentally and is the focus of the studies below. The $\mu^-\rho^+$ and $e^-\pi^+$ final states provide additional experimental signatures that extend the sensitivity and could be used to constrain additional parameter space.

Assuming a branching fraction 10^{-12} and a factor 10^{-4} from the lifetime, an experiment to detect $N_{2,3}$ would require more than 10^{16} D mesons in order to fully explore the parameter space with $M < 2$ GeV. Preliminary studies of an experimental design were described in Ref. [46].

3 Experimental status and cosmological constraints

The region of the lifetime-mass (τ, M_N) plane consistent with the cosmological constraints is shown in Fig. 2. Figure 4 shows the allowed region in the (U^2, M_N) plane, given the constraints from particle physics experiments. For all points in Fig. 4 below the line marked “Seesaw”, the mixing of the HNL with active neutrinos becomes too weak to produce the observed pattern of neutrino flavour oscillations. Cosmological considerations result in additional limits. If the HNLs are required

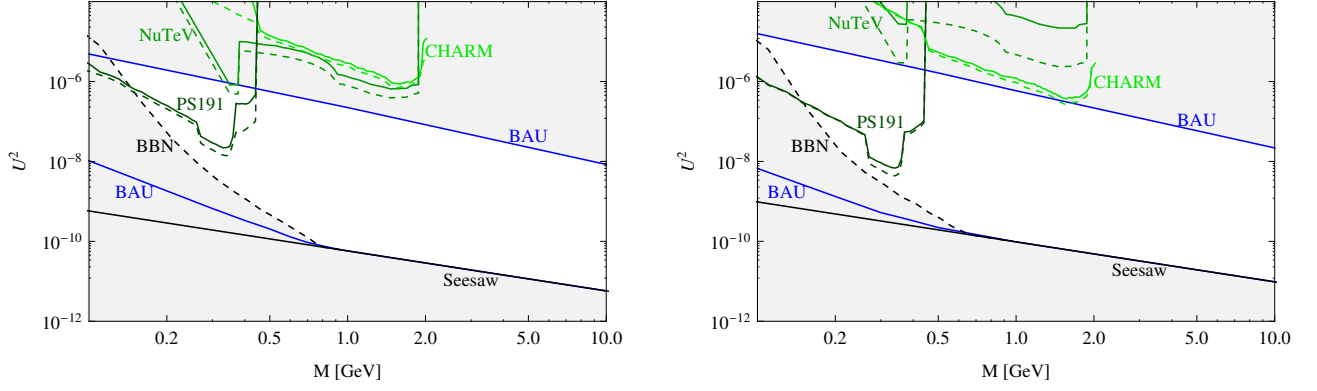


Figure 4: Current bounds on the parameters of the degenerate HNLs, $N_{2,3}$ in the (U^2, M_N) plane from cosmological considerations and neutrino mixing together with limits from previous experimental searches (the solid and dashed lines indicate the dependence of these regions on the pattern of HNL mixing with the electron, muon and tau-neutrino). Figures taken from Ref. [45]. A normal mass hierarchy of the neutrinos is shown on the left and an inverted hierarchy on the right.

to provide a mechanism for baryogenesis, their coupling with matter should be sufficiently weak such that they lie below the upper line marked “BAU”. A HNL with the parameters to the left of the “BBN” line would live sufficiently long in the early Universe to result in an overproduction of primordial Helium-4 in Big Bang Nucleosynthesis [47, 48]. The regions excluded by the CHARM [49], CERN PS191 [50] and NuTeV [51] experiments are also shown. Limits by BEBC [52] and CCFR [53] are not shown in Fig. 4. A detailed discussion of the experimental constraints (including also those from peak search experiments [54]) is presented in Refs. [9, 55, 56].

The combined experimental and theoretical constraints imply that the HNLs must have masses larger than approximately 100 MeV. The domain of masses accessible by the present experiment, i.e. masses below those of charm mesons, naturally appears under the assumption that the observed hierarchy in the masses of the different generations of quarks and charged leptons is preserved in the Majorana sector of the theory.

4 Experimental set-up

The proposed experiment will use a 400 GeV proton beam on a fixed target to produce a large number of charm mesons. The HNLs from charm meson decays have a significant polar angle with respect to the beam direction, ≈ 50 mrad on average, as shown in Fig. 5. In order to maximise the geometric acceptance for a given transverse size of the detector, the detection volume must therefore be placed as close as possible to the target.

The production of the charm mesons is accompanied by copious direct production of pions, kaons and short-lived light resonances. The subsequent decays of these particles would result in a large flux of muons and neutrinos. To minimise these decays, a combination of a target and a hadron absorber of a few metres length, both made of as dense a material as possible, is required. To reduce the detector occupancy and backgrounds induced by the residual muon flux, a muon shield is required downstream of the hadron absorber. The experimental set-up must therefore balance the opposing requirements of locating the detector as close as possible to the target and of accommodating a sufficiently long muon shield upstream of the fiducial volume of the detector to reduce muon-induced backgrounds.

The detector must be able to reconstruct the final state particles from $N \rightarrow \mu^- \pi^+$ decays,² identify

²Henceforth, the notation N will be used to indicate $N_{2,3}$.

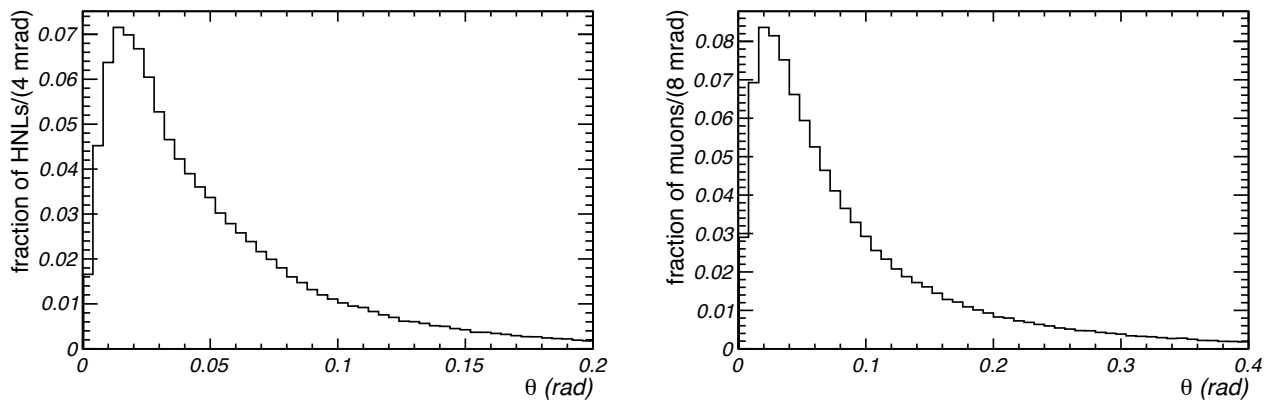


Figure 5: Polar angle distribution (left) of the HNLs and (right) of the muons and pions from the decay $N \rightarrow \mu^- \pi^+$ in simulated HNL decays with $M_N = 1$ GeV.

muons, and determine the $\mu^- \pi^+$ invariant mass and parent particle flight direction with sufficient resolution to reject backgrounds. To be sensitive to the decays $N \rightarrow e^- \pi^+$, $N \rightarrow e^- \rho^+$ and $N \rightarrow \mu^- \rho^+$ in addition to the $N \rightarrow \mu^- \pi^+$ decay, a magnetic spectrometer, an electromagnetic calorimeter and a muon detector are mandatory.

The background neutrino flux and the residual muon flux in the detector constitute crucial parameters in the design of the experiment. Interactions of neutrinos inside the fiducial volume can mimic signal events, in particular via charged-current interactions of muon-neutrinos. This motivates evacuating the fiducial volume to a level where such background events are negligible (see Section 5).

Interactions of neutrinos and muons in the material near the fiducial volume, can produce long-lived V^0 mesons, such as neutral kaons, which can decay in the detector fiducial volume and mimic signal events. To suppress neutrino-induced V^0 background events from the downstream end of the muon shield, the neutrino flux from light meson decays must be minimised at the source. This is achieved by the use of target and hadron absorber materials with the smallest possible interaction length. In addition, the muon shield must be sufficiently long to reduce muon-induced V^0 backgrounds to a level that is comparable to or smaller than the background from neutrinos. Shielding against cosmic rays is not required and the detector could therefore be located in an open space. A description of the proposed beam line and detector design is given below.

4.1 Beam line design

The SPS beam energy, beam intensity and the flexibility of the time structure offer a perfectly suitable production facility for the proposed experiment. The recently completed CERN Neutrinos to Gran Sasso (CNGS) programme made use of 400 GeV protons from the SPS over a nominal year with 200 days of operation, 55% machine availability, and 60% of the SPS supercycle. This produced a total of 4.5×10^{19} protons on target per year. The experiment described here assumes the same fraction of beam time as CNGS and the current SPS performance. In particular, the preliminary investigation of the operational mode assumes minimal modification to the SPS, maximises the use of the existing transfer lines and is compatible with the operation of both the LHC and the North Area fixed target programmes as they are currently implemented.

Increased experimental reach could come as a by-product of a future SPS upgrade from a proton spill intensity of about 4.5×10^{13} protons per pulse to 7.0×10^{13} protons per pulse. The design of the proposed experiment aims at taking advantage of such an upgrade but the experiment does not rely on it.

4.1.1 Beam extraction and proton target

From the general considerations given above, the experimental requirements favour the choice of a relatively long extraction to reduce the detector occupancy per unit time, and to allow a simple target design based on dense materials. At the same time, the extraction type should not affect significantly the SPS cycle time as compared to CNGS, and should respect the constraints on the activation levels in the extraction region and the risk of damage to the extraction septum. Several options exist, all of which may be acceptable from the point of view of the experiment, but the optimal choice requires further study:

- Slow extraction with a spill length of 1.2 s. This would mean a 7.2 s SPS spill cycle, and consequently a reduction of the number of protons on target by 10%;
- Fast non-coherent resonant extraction of $O(1\text{ ms})$;
- Fast extraction similar to that of CNGS of $O(10\text{ }\mu\text{s})$.

The first two options involve extraction with the SPS RF system OFF and the beams debunched. This produces a quasi-continuous spill that is compatible with a continuous detector readout, as described in Section 4.2.2. The first two extraction methods result in a lower detector occupancy.

With lifetimes of $\sim 10^{-12}\text{ s}$, the dominant fraction of D mesons decay before interacting in the target, regardless of the target material. However, the flux of secondary pions and kaons, which give rise to a substantial muon flux from decays in flight, can be greatly reduced by the use of a dense target material with a short interaction length. For example, the use of tungsten, rather than graphite, reduces the number of decaying pions and kaons by an order of magnitude. A 50 cm long tungsten target would suffice. However, the beam energy density must then be diluted in order to avoid destructive thermal shock waves in the target and to allow effective heat extraction. It may be possible to extract the deposited beam energy using water cooling.

Since the neutrinos produced in charm decays, which can mix with HNLs, have in any case a relatively high transverse momentum (see Fig. 5), there is no requirement to have a small beam spot. The beam line design can then be driven purely by the technical requirements and constraints. For the same reason, the experiment does not impose stringent constraints on the optical parameters of the extracted beam. The dilution of the beam energy deposition mentioned above may therefore be obtained by allowing the transverse size of the beam to increase in a dedicated section of the primary beam line, and by using a combination of orthogonally deflecting kicker magnets to produce a Lissajous sweep across the target, similar to the LHC beam dump. Preliminary investigation shows that it should be possible to achieve a beam spot size of about 5 mm on the target and a sweep diameter of several centimetres, with the only constraint being a beam divergence less than the natural divergence of the produced HNLs. Beam losses in the straight section leading to the target must be minimised and monitored to reduce the background neutrino flux.

The use of a slow extraction would simplify the target design. To prevent damage to the target caused by possible failures in the beam line, the beam extraction would need to be interlocked with the magnet currents in the dedicated transfer line.

The proton target will be required to withstand a beam power of 750 kW, corresponding to 7×10^{13} protons per 6 s at 400 GeV. Detailed thermo-mechanical studies will be required in order to produce a technical design.

4.1.2 Hadron absorber

To stop the remaining secondary pions and kaons before they decay, a hadron absorber will immediately follow the target. By surrounding the target, the absorber will also stop pions and kaons at large angles

which may otherwise produce muons that enter the fiducial volume due to large angle scattering. The absorber will also provide the first level of lateral radiation shielding, as well as absorbing the residual non-interacting protons ($\sim 1\%$ of the incident proton flux) and the electromagnetic radiation generated in the target. The physical dimensions of the absorber are driven by the radiological requirements on the muon shield (see Section 4.1.3 below). As part of the absorber, a concrete shielding wall will close-off the target bunker volume from the downstream muon shield tunnel.

4.1.3 Muon shield

The muon flux after the hadron absorber is estimated from a sample of 10^9 pp events generated with PYTHIA with a proton beam energy of 400 GeV and a fixed proton target. The prompt component of the muon flux originates from the electromagnetic decays of meson resonances, mainly η , ρ , ϕ , ω . The non-prompt component originates mainly from the decay in flight of charged pions and kaons. For the present estimates, only the decays of primary pions and kaons are considered as non-prompt sources. Secondary, tertiary, or higher order pion or kaon decays should give a softer momentum spectrum that is more easily attenuated than the high-energy primary pion and kaon decays that drive the requirement on the muon shield length. The exact radial extent of the muon shield will be defined based on a detailed simulation to ensure that the muons from higher order interactions, which generally have larger polar angles, are also absorbed.

The dense target and the hadron absorber described above will be designed to stop all hadrons. However, a fraction $\mathcal{B}_\mu \lambda_{\text{int}}/\lambda_{\text{dec}}$ of the hadrons entering the absorber will decay into muons before interacting, where λ_{int} is the interaction length of hadrons in the hadron absorber; $\lambda_{\text{dec}} = \tau p/M$ is the decay length of the hadron and τ , p and M are the hadron lifetime, lab momentum and rest mass; and \mathcal{B}_μ is the branching fraction for the decay of the hadron to muons (100% for $\pi^+ \rightarrow \mu^+ \nu_\mu$ and 63% for $K^+ \rightarrow \mu^+ \nu_\mu$, other muon-producing decay channels are neglected). A cross-check with the muon fluxes observed in the CHARM “beam dump” experiment [57] indicates that the above method for estimating the “first-generation” muon flux gives the correct order of magnitude. The resulting muon flux is shown as a function of the muon momentum in Fig. 6. The muons from charm decays represent a negligible fraction of the total muon flux.

Figure 6 indicates that if a shield were put in place to stop muons below 350 GeV, the muon flux would be reduced by about seven orders of magnitude to $\mathcal{O}(1)$ muon per 10^9 protons on target. However, the muon-induced V^0 production rate from nuclei would still be larger than that of neutrino interactions that is computed in Section 5. Therefore, the experiment will use a muon absorber that nominally stops muons with energies of up to 400 GeV, which requires a length of 52 m of uranium (or 54 m of tungsten) [58].

4.1.4 Potential experimental site

The final configuration of the beam line and detector will be based on an optimisation of the proton spill duration, the target design, the hadron absorber and the muon shield lengths, and the number of protons on target.

The general beam line layout as described above is shown in Fig. 7. The proposed beam line arrangement consists of a proton beam impinging on a ~ 0.5 m long target, followed by a hadron absorber of ~ 3 m length, a shielding wall to confine air and radiation, and a ~ 52 m long uranium or tungsten muon absorber enclosed in iron and concrete.

The experiment requires a new switching section from an existing beam line, which can be very similar to the one already used for the CNGS facility. A short section of transfer line, consisting almost entirely of drift length to allow the beam energy density to be reduced, will then bring the high

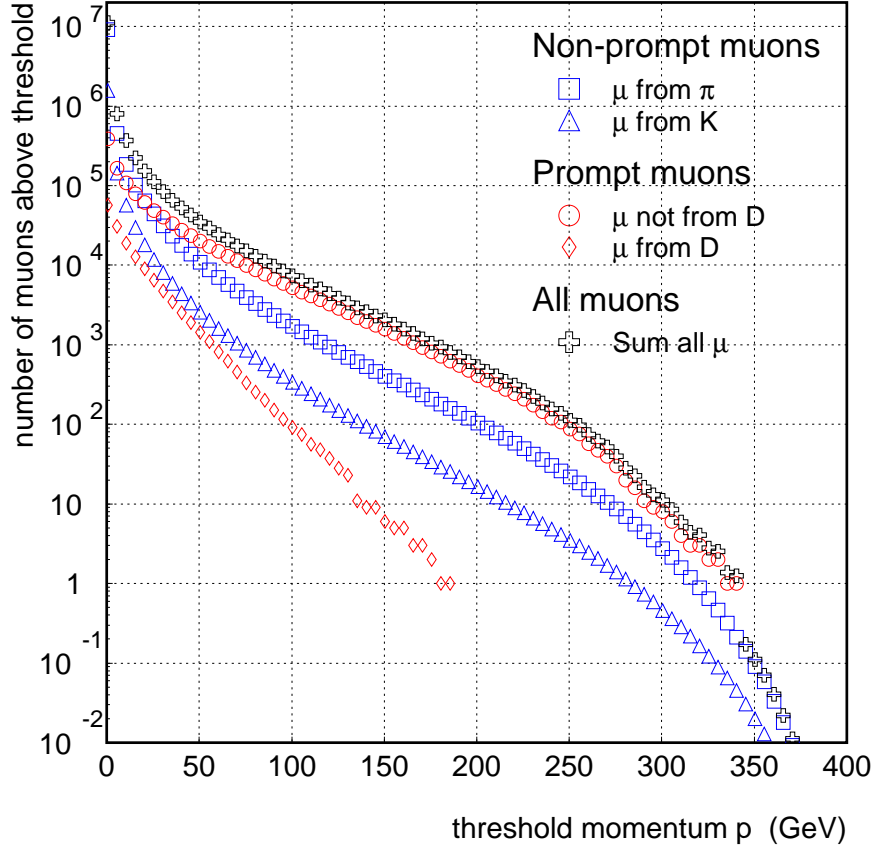


Figure 6: Estimated muon fluxes after a hadron absorber based on 10^9 pp events generated with PYTHIA with a proton beam of 400 GeV and a fixed proton target (see text for details). The total flux of first-generation muons above a given momentum is shown.

energy protons to the target bunker that contains the target and the hadron absorber. The site of the experiment should be such that it allows use of existing infrastructure. In particular, the site will need to be provisioned with the equipment to handle air and water activation, to comply with radiation protection standards. The site should also be well within the CERN boundaries. Both construction and operation of the beam line and the detector can be such that the interference caused to running facilities is minimised.

Based on these requirements and constraints, the North Area could provide a suitable location with a relatively short transfer line of a few hundred metres, branching-off from TT20, with a new beam splitting near to the TDC2 splitter area. The beam deflection could then be arranged to allow the dedicated transfer line to point to a target bunker at sufficient depth and distance from the TCC2 target area to minimise the excavation in activated soil. Soil tests will be needed to determine the exact location. A 60m trenched tunnel after the target bunker would allow the installation of the muon shield, and an area at relatively low elevation just before the North Area hall would provide a suitable site for the location of the surface detector building. The location of the proposed target bunker near to the TCC2 target area suggests that it may be possible to benefit from the general refurbishments that are already foreseen for the current target area in terms of activated water and air treatment.

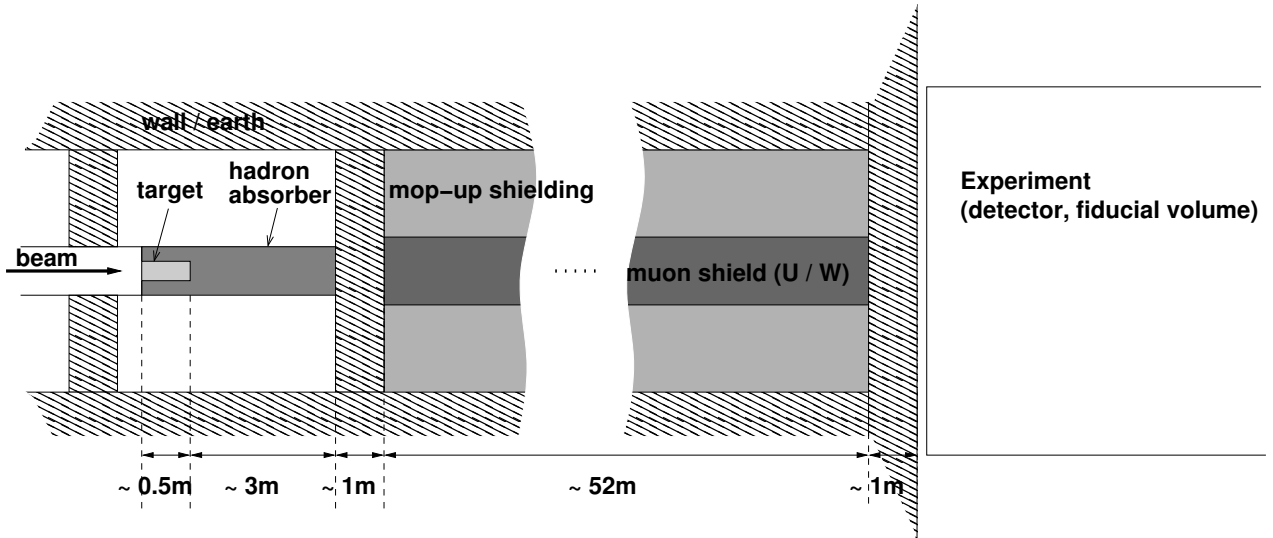


Figure 7: Schematic view of the target, hadron absorber and muon shield in front of the experiment. The total length from the target to the entrance of the fiducial volume is ~ 60 m.

4.2 Detector

The detector consists of a long decay volume followed by a spectrometer. For a given detector length, the detector diameter should be maximised. In the discussion below the 5 m aperture of the LHCb spectrometer [59] is taken as a realistic scale.

Figure 8 shows a scan of the length of the detector for both a single detector element and for two longitudinally arranged detector elements. For a given HNL lifetime and detector aperture, the number of HNLs decaying in the apparatus with the decay products going through the spectrometer saturates as a function of the length of the detector. The use of two magnetic spectrometers increases the geometric acceptance by 70% compared to a single element. Therefore, the proposed detector will have two almost identical detector elements as depicted in Fig. 9. A diagram of a single detector element is also shown in Fig. 10.

To reduce to a negligible level the background caused by interactions of neutrinos with the remaining air inside the decay volume, a pressure of less than $\sim 10^{-2}$ mbar will be required (see Section 5). Each detector element therefore consists of a ~ 50 m long cylindrical vacuum vessel of 5 m diameter. The first ~ 40 m constitute the decay volume and the subsequent 10 m are used for the magnetic spectrometer. The combined calorimeter and muon detector have a length of 2 m.

The magnetic spectrometer includes a 4 m long dipole magnet, two tracking layers upstream of the magnet, and two tracking layers downstream of the magnet (see Fig. 9). For the required level of vacuum, the tracking chamber thickness and resolution are matched to give a similar contribution to the overall spectrometer resolution (see Fig. 11). Using straw tubes with $\sim 120 \mu\text{m}$ resolution and with 0.5% X/X_0 , like those presently being produced for the NA62 experiment [60], simulation studies indicate that 2.5 m is required between tracking chambers, giving ~ 10 m length for each magnetic spectrometer.

An electromagnetic calorimeter is located behind each vacuum vessel for π^0 reconstruction and lepton identification. The calorimeter material is also part of the muon filter for the muon detector, which consists of an iron wall followed by a tracking station. An additional tracking station at the beginning of each decay vessel will be used to veto charged particles entering the fiducial volume. These stations will also reject upstream neutrino interactions.

For a mass $M_N = 1 \text{ GeV}$, 75% of the $\mu^- \pi^+$ decay products have both tracks with momentum $p < 20 \text{ GeV}$. The momentum and hence mass resolution scales with the integrated field of the magnets.

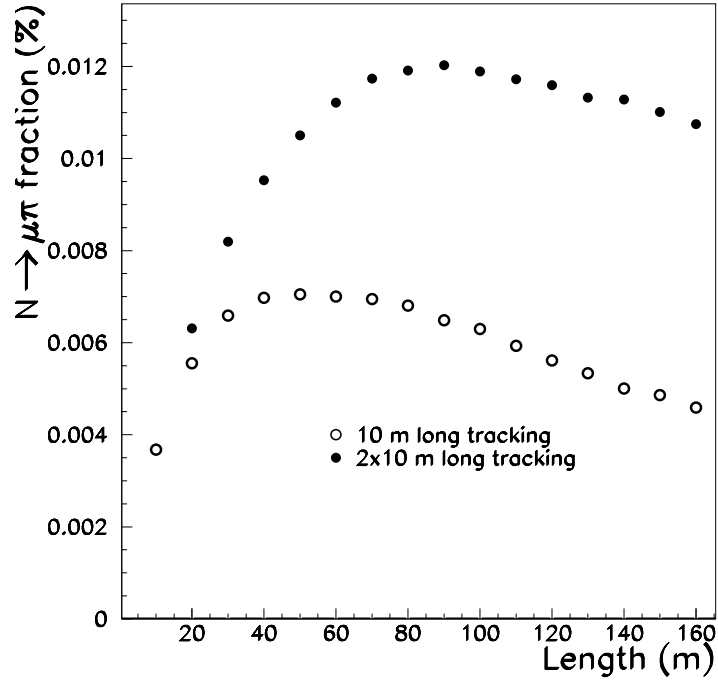


Figure 8: Fraction of HNL in the detector acceptance as a function of the length of the fiducial volume. Open circles: a single spectrometer following a fiducial volume of a given length. Full circles: two spectrometers in series, each following a fiducial volume of half the given length. The spectrometer length is fixed to 10 m.

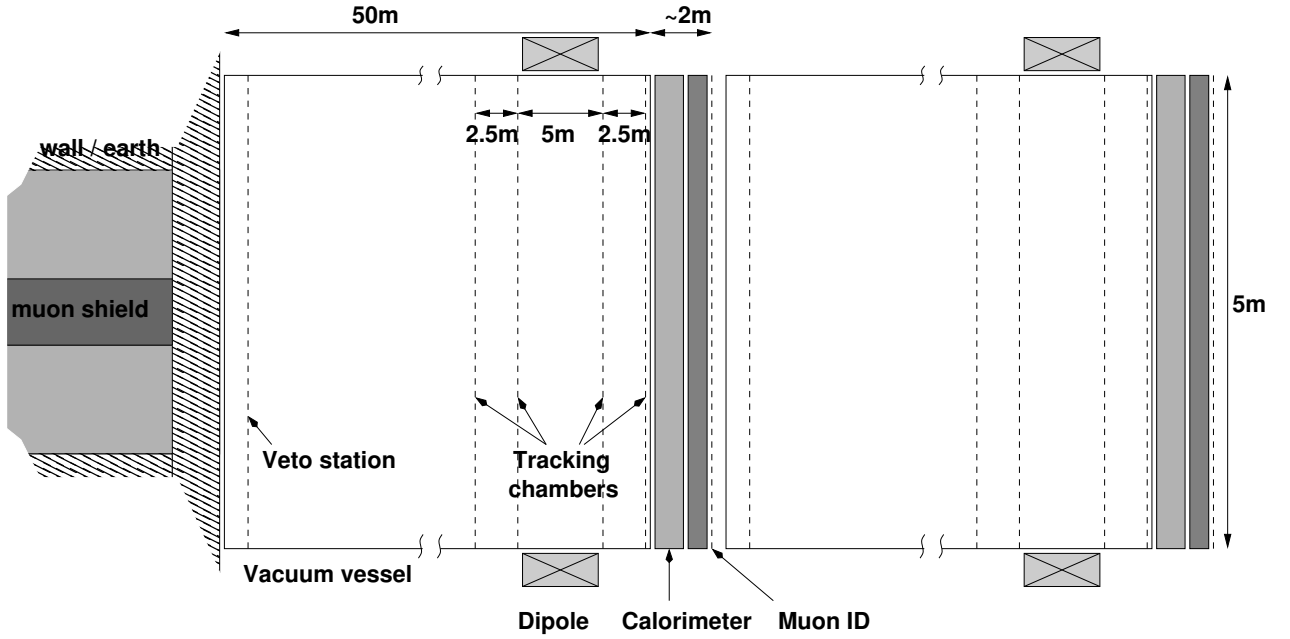


Figure 9: Two-dimensional view of the fiducial volume and detector arrangement.

A 0.5 Tm field integral results in a mass resolution of ~ 40 MeV for $p < 20$ GeV tracks (see Fig. 12). For a 1 GeV HNL this provides ample separation between the signal peak and the high mass tail of partially reconstructed $K_L^0 \rightarrow \pi^+ \mu^- \nu$ decays. Further optimisation of the magnetic field will need to take into account the shape of the high mass tail from such decays which may enter the signal mass window.

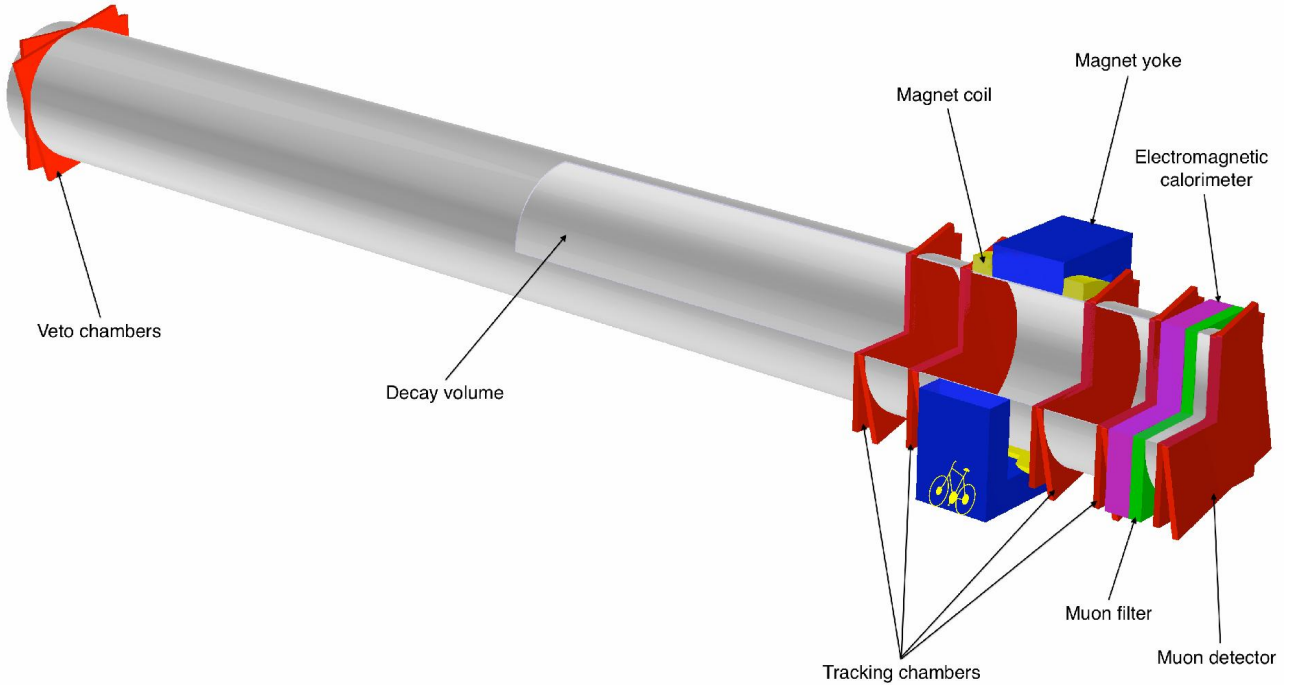


Figure 10: Three-dimensional sketch of the fiducial volume and detector arrangement.

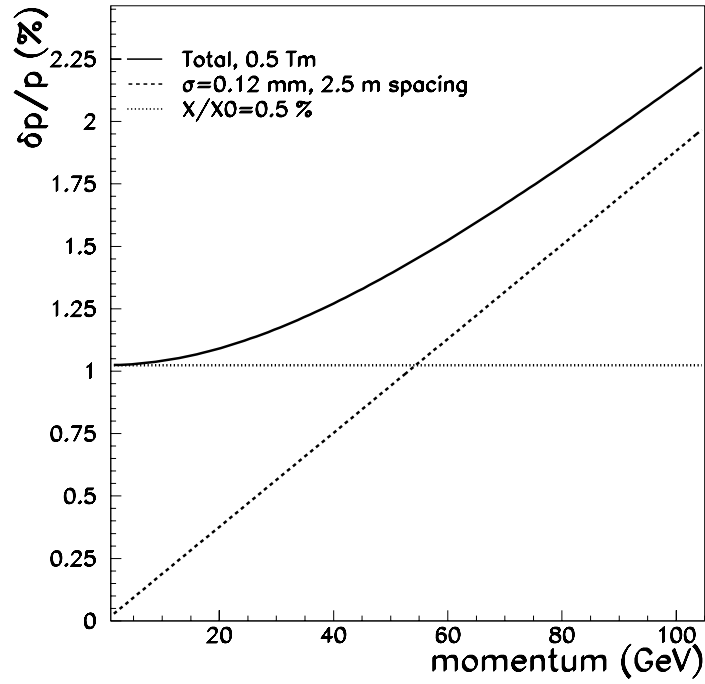


Figure 11: Estimated momentum resolution of the spectrometer (solid line) with separate contributions from multiple scattering (dotted line) and chamber resolution (dashed line).

4.2.1 Magnet

A feasibility study of a dipole magnet, similar to the LHCb magnet [59], with a free aperture of almost 16 m^2 and a field integral of $\sim 0.5 \text{ Tm}$, has been conducted.

Figure 13 shows a sketch of a magnet which fulfills the requirements of the proposed experiment [61].

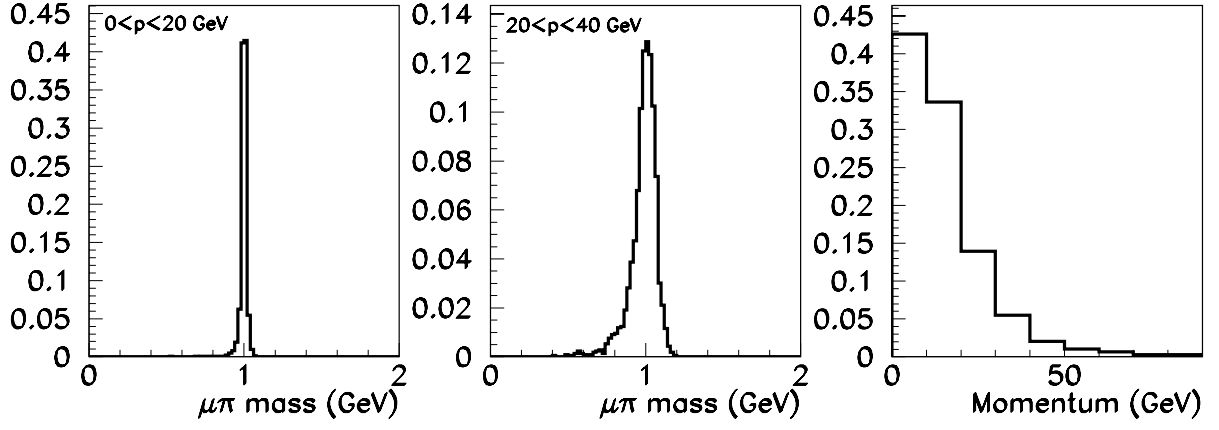


Figure 12: Simulated mass resolution for $N \rightarrow \mu^- \pi^+$ decay products with various momenta in the left and middle panels and the momentum spectrum of the decay products in the rightmost panel. The momentum window indicated is for the measured momenta and is required for the harder of the two decay products. A HNL with mass 1 GeV is assumed.

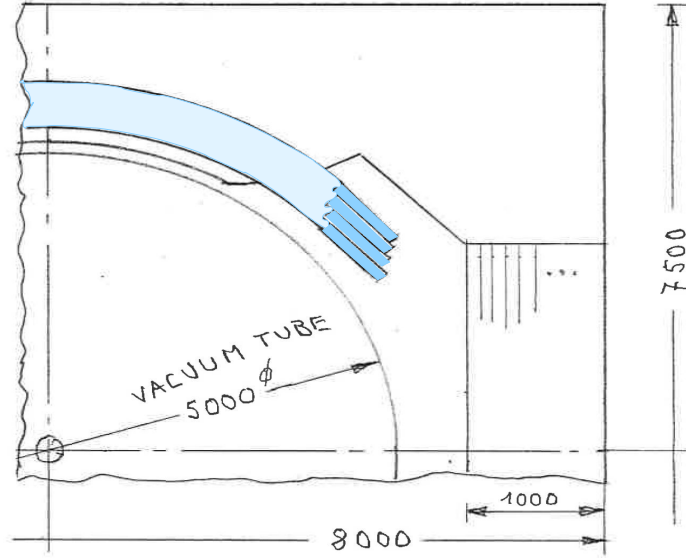


Figure 13: Sketch of a quarter of the dipole magnet viewed along the direction of the beam. The Al coil is shown in blue. The units are mm.

With a yoke with outer dimension of $8.0 \times 7.5 \times 2.5 \text{ m}^3$, and two Al-99.7 coils, the proposed magnet provides a peak field of $\sim 0.2 \text{ T}$, and a $\int B dL \approx 0.5 \text{ Tm}$ over a length of $\sim 5 \text{ m}$. For comparison, the LHCb magnet mentioned above contains $\sim 40 \%$ more iron for its yoke, and dissipates three times more power.

4.2.2 Synergy with other detectors

The proposed experiment will require two $\sim 50 \text{ m}$ long, 5 m diameter vacuum tanks each of which will be similar to that used in the NA62 experiment [60]. The $\sim 10^{-2} \text{ mbar}$ vacuum required to suppress neutrino interactions (see Section 5), is several orders of magnitude less demanding than the pressure used in the NA62 vacuum tank ($< 10^{-5} \text{ mbar}$) and should therefore not represent a technological challenge.

The tracking stations of the magnetic spectrometer must provide good spatial resolution and minimise the contribution from multiple scattering. The NA62 straw tracker tubes [60], which are man-

ufactured from thin polyethylene terephthalate (PET), are ideal to meet both of these goals. Gas tightness of these tubes has been demonstrated in long term tests and the mass production procedure is also well established.

The reconstruction of π^0 mesons and the identification of electrons would be required to reconstruct decays such as $N \rightarrow \rho^+(\rightarrow \pi^+\pi^0)\mu^-$ and $N \rightarrow e^-\pi^+$. An electromagnetic calorimeter with a modest energy resolution will therefore substantially improve the discovery potential of the proposed experiment. The LHCb shashlik calorimeter has demonstrated an energy resolution of $\frac{\sigma(E)}{E} < 10\%/\sqrt{E} \oplus 1.5\%$, which is comparable to the momentum resolution of the proposed magnetic spectrometer in the 10 to 20 GeV energy range. The shashlik technology also provides an economical solution with fine granularity, as well as time resolution better than a few ns, which will be needed to correlate the calorimeter and tracker information.

The SPS provides a quasi-continuous flux of protons on target over its extraction period. A dead-timeless readout system such as that envisaged for the LHCb Upgrade [62] would suffice for the proposed experiment. This readout system will record data continuously in 25 ns time-slices. The data will be pushed out to read-out boards which in turn will push the data to a PC-farm to perform the event building. Tracks with matching times will be combined to form two-prong vertices, and events with good vertices will be maintained for further analysis. This part of the selection will be executed on-line in the event building farm to reduce the data storage rate to a negligible level. It is estimated that storage of ~ 10 TB/year would be required.

5 Background

The muon shield described above is designed to stop muons with momenta of up to 400 GeV, thus reducing muon-induced backgrounds to a negligible level.

The rate of charged-current neutrino interactions (CC) occurring at the downstream end of the muon shield is estimated by extrapolating from a measurement by CHARM [63], which used 400 GeV protons impinging on a Cu target. To extrapolate this measurement to the proposed geometry, the angular and momentum distributions of the neutrinos are simulated using PYTHIA [64]. This results in an expected CC rate in the last interaction length of the muon shield of 260×10^3 per 2×10^{20} protons on target if a Cu target were used. As a cross-check GEANT [65] is used to simulate the neutrino spectrum produced by a 400 GeV proton beam on a Cu target. This yields a CC rate four times larger than the estimate based on the CHARM data.

Replacing the Cu target by a W target lowers the CC rate by 45%. The neutrinos from the GEANT simulation using a W target are passed to GENIE [66] to simulate the CC and neutral-current (NC) neutrino interactions in the muon shield. This yields a CC(NC) rate of $\sim 600(200) \times 10^3$ per interaction length per 2×10^{20} protons on target. Conservatively, this rate is used to evaluate the background.

Neutrino interactions in the decay volume could be a source of background. In a decay volume filled with air under atmospheric pressure, the above rate translates into $\sim 20 \times 10^3$ neutrino interactions per 2×10^{20} protons on target. A pressure in the decay volume of 0.01 mbar reduces this rate to a negligible level.

Another source of background is the rate of the neutrino interactions that occur in the muon shield just upstream of the decay volume. A combination of GEANT and GENIE is used to predict that in $\sim 10\%$ of the neutrino interactions a Λ or K^0 will be produced. This prediction is consistent with measurements by NOMAD [67]. In the first 5 m of the decay volume two-prong vertices are mainly from Λ and K_S^0 decays. For the remaining 35 m of the decay volume 95% of two-prong vertices originate from K_L^0 decays. Requiring one of the two decay tracks to be identified as a muon, yields ~ 150 two-prong vertices in 2×10^{20} protons on target. Owing to their different kinematics, the geometrical

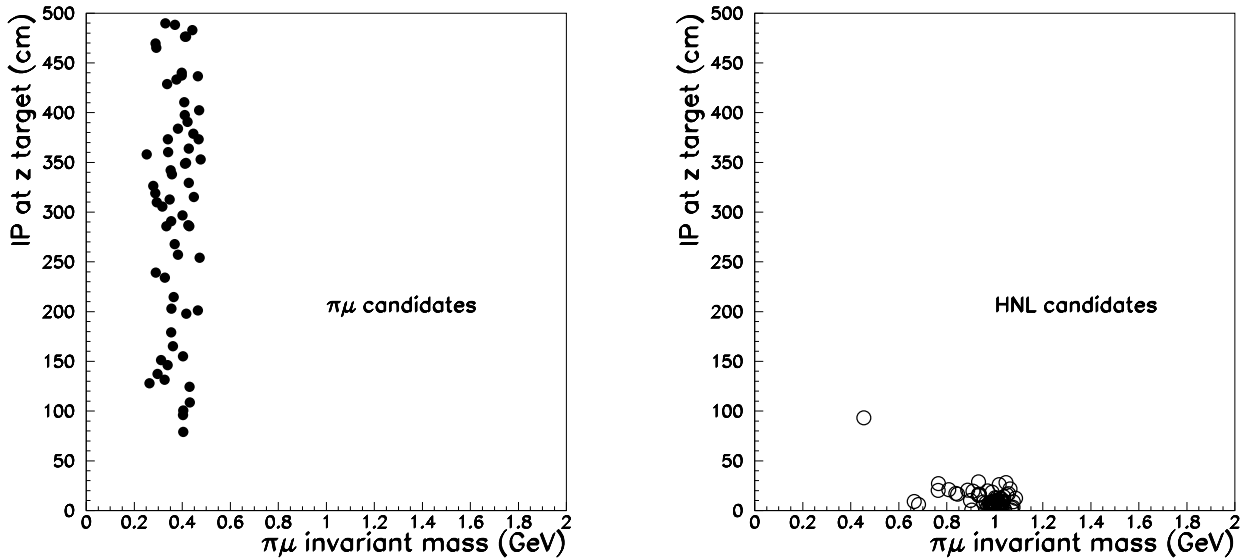


Figure 14: Invariant mass of two-prong candidates and their distance of closest approach (IP) to the W target (left) for background events generated with GEANT and GENIE, and (right) for $N \rightarrow \mu^- \pi^+$ with a 1 GeV invariant mass for the signal.

acceptance of K_L^0 decay products is significantly smaller than that of HNL decay products. Figure 14 shows the invariant mass of these candidates together with their distance of closest approach (IP) when extrapolated back to the W target. Requiring $IP < 1$ m reduces this background to a handful of candidates for 2×10^{20} protons on target, while the IP of all signal candidates is below 1 m. The IP of candidates will also be used to reject possible background induced in neutrino interactions in the surrounding material, like the vacuum tank or the floor, and from cosmic rays.

Backgrounds that originate from neutrino interactions could be vetoed by detecting the associated activity produced in the associated shower, especially the lepton in CC interactions. This signature has not been exploited yet in the above yields and could be used to reduce the background to a negligible level. More detailed simulation studies will be undertaken to optimise the position of the veto stations at the entrance of the decay volume. If shown to be advantageous, the last interaction lengths of both the muon shield and the muon filter could be instrumented in order to detect the products of neutrino interactions.

%inputSensitivity

6 Expected event yield

The sensitivity of the proposed experiment depends on the final states used to reconstruct the signal decays and the pattern of couplings between the neutrino generations and the HNLs. The region in U_μ^2 that can be probed by the proposed experiment is conservatively estimated by assuming only the decay $N \rightarrow \mu^- \pi^+$ is used and considering the production mechanism $D \rightarrow \mu^+ N X$. The relationship between U_μ^2 and U^2 is discussed in Ref. [56]. As detailed in Section 3, the present strongest limits on U_μ^2 come from the CHARM experiment [49] and are at the 10^{-7} level for a mass of 1.5 GeV and a few times 10^{-6} for a mass of 1 GeV. The theoretically allowed region for U_μ^2 is between 10^{-7} and 10^{-11} .

The expected number of signal events for the proposed experiment is given by

$$n_{\text{signal}} = n_{\text{pot}} \times 2\chi_{c\bar{c}} \times \mathcal{B}(U_\mu^2) \times \epsilon_{\text{det}}(U_\mu^2), \quad (5)$$

where $n_{\text{pot}} = 2 \times 10^{20}$ is the total number of protons on target, $\chi_{c\bar{c}} = 0.45 \times 10^{-3}$ is the ratio of the $c\bar{c}$ production cross-section with respect to the total cross-section (the factor 2 accounts for the fact that charm is produced in pairs), ϵ_{det} is the total efficiency and \mathcal{B} is the product of the production and decay branching fractions of the HNLs. The quantity ϵ_{det} can be written as the product of the probability that the HNLs decay in the fiducial volume and the trigger and reconstruction efficiencies. The probability of decay is estimated with simulated events for different values of U_μ^2 and the efficiencies are assumed to be 100%. The dependence on the HNL lifetime introduces a U_μ^2 factor in ϵ_{det} . Since the quantities \mathcal{B} and ϵ_{det} each depend on a factor U_μ^2 , this results in an overall U_μ^4 dependence.

Assuming $U_\mu^2 = 10^{-7}$, a HNL mass of 1 GeV, $\mathcal{B} = 8 \times 10^{-10}$, $\tau = 1.8 \times 10^{-5}$ s and $\epsilon_{\text{det}} = 8 \times 10^{-5}$, ~ 12000 fully reconstructed $N \rightarrow \mu^- \pi^+$ events would be observed, four orders of magnitudes larger than the number that would be expected in the CHARM experiment. Considering a point in the cosmologically favoured region with $U_\mu^2 = 10^{-8}$, $\tau = 1.8 \times 10^{-4}$ s and $M = 1$ GeV, 120 fully reconstructed $N \rightarrow \mu^- \pi^+$ events would be expected in the proposed experiment.

The electromagnetic calorimeter allows the reconstruction of decay modes with a neutral pion in the final state such as $N \rightarrow \mu^- \rho^+$, where the $\rho^+ \rightarrow \pi^+ \pi^0$, allowing the signal yields to be doubled. Channels with electrons, such as $N \rightarrow e^- \pi^+$, could also be studied, allowing a further increase in the yields and the parameter U_e^2 to be probed. Other decay channels with a SM neutrino in the final state, e.g. $N \rightarrow l_1^- l_2^+ \nu$, are more challenging to select, since the invariant mass will have a broad distribution but could be separated from the background by using particle identification information.

Both the background levels and the total neutrino flux will be measured by the experiment itself. The neutrino flux from charm-meson decays is more difficult to obtain experimentally. A study of the p_T distribution of neutrino events in the calorimeter together with existing 400 GeV pCu data [63] and a detailed simulation will provide a normalisation.

In summary, for a HNL mass below 2 GeV the proposed experiment has discovery potential for the cosmologically favoured region with U_μ^2 between 10^{-7} and a few times 10^{-9} .

6.1 Comparison with other facilities

Fixed target experiments of the type proposed could be performed using both the Fermilab and KEK proton beams. The beams considered are the 800 GeV and 120 GeV FNAL beams with 1×10^{19} protons on target and 4×10^{19} protons on target, respectively; and the KEK 30 GeV beam with 1×10^{21} protons on target.

At FNAL, the 800 GeV beam would give a similar HNL flux to that of the proposed SPS experiment, i.e. the lower proton intensity would be approximately compensated by the increase in the charm cross-section at higher energy [68]. However, a significantly longer muon filter would be required due to the higher beam energy, which would be much more challenging, leading to a significant loss of acceptance.

The FNAL 120 GeV beam would have a factor ten lower event yield than in the proposed SPS experiment, while the KEK beam would have a factor 1.5–2 lower yield, the latter estimate has a large uncertainty due to the poor knowledge of the charm cross-section at low energy.

The sensitivity of a colliding beam experiment at the CERN LHC is estimated assuming a luminosity of 1000 fb^{-1} and an energy of 14 TeV, as is foreseen in three to four years of running for the high luminosity upgrade. The HNL decay volume is taken to be located 60 m away from the interaction region and 50 mrad off-axis, in order to avoid the LHC beam line. The overall HNL event yield would be a factor approximately 200 smaller than in the proposed SPS experiment.

Although masses of the HNLs are expected to be around the GeV-scale, it is possible that they are heavier than D mesons. If the HNLs are lighter than ~ 5 GeV, they can be produced in beauty hadron decays. The most copious HNL production mechanism with B mesons would be the semileptonic $B \rightarrow D l N$ decays and the total available mass would therefore be restricted to less than ~ 3 GeV.

The reduced cross-section for the production of beauty mesons with respect to charm mesons means that the limits that could be derived from a dedicated experiment at the LHC would be about four orders of magnitude weaker than those from charm decays. Such limits would then be comparable to the upper limits from the theoretical consideration of the baryon asymmetry.

The SPS at CERN is therefore the ideal facility to conduct the proposed experiment to search for HNLs.

7 Conclusion

The proposed experiment will search for New Physics in the largely unexplored domain of new, very weakly interacting particles with masses below the Fermi scale. This domain is inaccessible to the LHC experiments and to comparable experiments at other existing facilities.

The proposed detector is based on existing technologies and therefore requires no substantial R&D phase. A moderately sized collaboration could construct the proposed detector in a few years. The design of the beam line is challenging, in particular, the beam extraction and beam target, as well as the radiological aspects require further study. The solutions proposed are being actively discussed with machine experts.

The impact that a discovery of a HNL would have on particle physics is difficult to overestimate. In short, it could solve two of the most important shortcomings of the SM: the origin of the baryon asymmetry of the Universe, the origin of neutrino mass. In addition, the results of this experiment, together with cosmological and astrophysical data, could be crucial to determine the nature of dark matter.

Acknowledgements

We are grateful to G. Arduini, M. Calviani, D. Grenier, E. Gschwendtner and H. Vincke for useful discussions and valuable input on the beam line and the target. We would like to thank F. Rademakers for providing the three dimensional sketch of the experiment. W. Flegel is warmly acknowledged for adapting the design of the LHCb magnet to our needs. We are grateful to S. Gninenko and A. Rozanov for stimulating discussions and to E. van Herwijnen for setting up our web site.

References

- [1] G. Aad *et al.*, ATLAS collaboration, Phys. Lett. **B 716** (2012) 1, arXiv:hep-ex/1207.7214; ATLAS collaboration, <http://cds.cern.ch/record/1523727>.
- [2] S. Chatrchyan *et al.*, CMS collaboration, Phys. Lett. **B 716**, (2012) 30, arXiv:hep-ex/1207.7235; CMS collaboration, <http://cds.cern.ch/record/1542387>.
- [3] F. Cerutti, Talk at EPS HEP Conference, Stockholm, 2013, <https://cds.cern.ch/record/1598145>.
- [4] J. Ellis *et al.*, Phys. Lett. **B 679** (2009) 369, arXiv:hep-ph/0906.0954.
- [5] D. Buttazzo *et al.*, arXiv:hep-ph/1307.3536.
- [6] F. Bezrukov, M.Y. Kalmykov, B.A. Kniehl and M. Shaposhnikov, JHEP **10** (2012) 140, arXiv:hep-ph/1205.2893.
- [7] T. Asaka, S. Blanchet and M. Shaposhnikov, Phys. Lett. **B 631** (2005) 151, arXiv:hep-ph/0503065.

- [8] T. Asaka and M. Shaposhnikov, Phys. Lett. **B 620** (2005) 17, arXiv:hep-ph/0505013.
- [9] D. Gorbunov and M. Shaposhnikov, JHEP **10** (2007) 015, arXiv:hep-ph/0705.1729.
- [10] B. Batell, M. Pospelov and A. Ritz, Phys. Rev. **D83** (2011) 054005, DOI:10.1103/PhysRevD.83.054005, arXiv:hep-ph/0911.4938.
- [11] D. S. Gorbunov, Nucl. Phys. B **602** (2001) 213, arXiv:hep-ph/0007325.
- [12] A. Dedes, H.K. Dreiner and P. Richardson, Phys. Rev. **D65** (2001) 015001, DOI:10.1103/PhysRevD.65.015001, arXiv:hep-ph/0106199.
- [13] A.E. Faraggi and M. Pospelov, Phys. Lett. **B458** (1999) 237, DOI:10.1016/S0370-2693(99)00557-2, arXiv:hep-ph/9901299.
- [14] S. N. Gninenko, Phys. Rev. Lett. **103** (2009) 241802, arXiv/hep-ph:0902.3802; S. N. Gninenko and D. S. Gorbunov, Phys. Rev. D **81** (2010) 075013, arXiv:hep-ph/0907.4666.
- [15] T.M. Aliev, A.S. Cornell and N. Gaur, JHEP **07** (2007) 072, DOI:10.1088/1126-6708/2007/07/072, arXiv:hep-ph/0705.4542.
- [16] F. Bergsma *et al.*, CHARM collaboration, Phys. Lett. **B 157** (1985) 458.
- [17] R.N. Mohapatra and P.B. Pal, World Sci. Lect. Notes Phys. **60** (1998) 1; World Sci. Lect. Notes Phys. **72** (2004) 1.
- [18] P. Minkowski, Phys. Lett. **B 67** (1977) 421. T. Yanagida, Progr. Theor. Phys. **64** (1980) 1103; M. Gell-Mann, P. Ramond and R. Slansky, in *Supergravity*, North Holland, Amsterdam, 1980; R.N. Mohapatra and G. Senjanovic, Phys. Rev. Lett. **44** (1980) 912.
- [19] M. Fukugita and T. Yanagida, Phys. Lett. **B 174** (1986) 45.
- [20] V.A. Kuzmin, V.A. Rubakov and M.E. Shaposhnikov, Phys. Lett. **B 155** (1985) 36.
- [21] F.R. Klinkhamer and N.S. Manton, Phys. Rev. **D 30** (1984) 2212.
- [22] G. Senjanovic, Riv. Nuovo Cim. **034** (2011) 1.
- [23] G.F. Giudice, in G. Kane and A. Pierce (eds.), *Perspectives on LHC physics* (2008) 155, arXiv:hep-ph/0801.2562.
- [24] A. Pilaftsis and T.E.J. Underwood, Nucl. Phys. **B 692** (2004) 303, arXiv:hep-ph/0309342.
- [25] A. Pilaftsis and T.E.J. Underwood, Phys. Rev. **D 72** (2005) 113001, arXiv:hep-ph/0506107.
- [26] E.K. Akhmedov, V.A. Rubakov and A.Y. Smirnov, Phys. Rev. Lett. **81** (1998) 1359, arXiv:hep-ph/9803255.
- [27] S. Dodelson and L.M. Widrow, Phys. Rev. Lett. **72** (1994) 17, arXiv:hep-ph/9303287.
- [28] X.-D. Shi and G.M. Fuller, Phys. Rev. Lett. **82** (1999) 2832, arXiv:astro-ph/9810076.
- [29] A. Boyarsky, O. Ruchayskiy and M. Shaposhnikov, Ann. Rev. Nucl. Part. Sci. **59** (2009) 191, arXiv:hep-ph/0901.0011.
- [30] R.E. Shrock, Phys. Rev. **D 24** (1981) 1232.

- [31] R.E. Shrock, Phys. Rev. **D 24** (1981) 1275.
- [32] M. Gronau, C.N. Leung and J.L. Rosner, Phys. Rev. **D 29** (1984) 2539.
- [33] L.M. Johnson, D.W. McKay and T. Bolton, Phys. Rev. **D 56** (1997) 2970, arXiv:hep-ph/9703333.
- [34] P.A.R. Ade *et al.*, Planck collaboration, arXiv:astro-ph/1303.5076.
- [35] A. de Gouvea, Phys. Rev. **D 72** (2005) 033005, arXiv:hep-ph/0501039.
- [36] A.A. Aguilar-Arevalo *et al.*, LSND collaboration, Phys. Rev. **D 64** (2001) 112007, arXiv:hep-ex/0104049.
- [37] A.A. Aguilar-Arevalo *et al.*, MiniBooNE collaboration, Phys. Rev. Lett. **110** (2013) 161801, arXiv:hep-ex/1207.4809; arXiv:hep-ex/1303.2588.
- [38] G. Mention *et al.*, Phys. Rev. **D 83** (2011) 073006, arXiv:hep-ex/1101.2755.
- [39] J.N. Abdurashitov *et al.*, Phys. Rev. **C 73** (2006) 045805, arXiv:nucl-ex/0512041.
- [40] J.N. Abdurashitov *et al.*, SAGE collaboration, Phys. Rev. **C 59** (1999) 2246, arXiv:hep-ph/9803418.
- [41] W. Hampel *et al.*, GALLEX collaboration, Phys. Lett. **B 420** (1998) 114.
- [42] F. Kaether *et al.*, Phys. Lett. **B 685** (2010) 47, arXiv:hep-ex/1001.2731.
- [43] M. Gonzalez-Garcia, M. Maltoni, J. Salvado and T. Schwetz, JHEP **12** (2012) 123, arXiv:hep-ph/1209.3023.
- [44] M. Drewes and B. Garbrecht, JHEP **03** (2013) 096, arXiv:hep-ph/1206.5537.
- [45] L. Canetti, M. Drewes, T. Frossard and M. Shaposhnikov, Phys. Rev. **D 87** (2013) 093006, arXiv:hep-ph/1208.4607; L. Canetti, M. Drewes and M. Shaposhnikov, Phys. Rev. Lett. **110** (2013) 6, 061801, arXiv:hep-ph/1204.3902.
- [46] D. Gorbunov and M. Shaposhnikov, Proposal submitted to European Strategy Group, 2012; S.N. Gninenko, D.S. Gorbunov and M.E. Shaposhnikov, Adv. High Energy Phys. **2012** (2012) 718259, arXiv:hep-ph/1301.5516.
- [47] A.D. Dolgov, S.H. Hansen, G. Raffelt and D.V. Semikoz, Nucl. Phys. **B 590** (2000) 562, arXiv:hep-ph/0008138.
- [48] O. Ruchayskiy and A. Ivashko, JCAP **10** (2012) 014, arXiv:hep-ph/1202.2841.
- [49] F. Bergsma *et al.*, CHARM collaboration, Phys. Lett. **B 166** (1986) 473.
- [50] G. Bernardi *et al.*, Phys. Lett. **B 166** (1986) 479; G. Bernardi *et al.*, Phys. Lett. **B 203** (1988) 332; F. Vannucci, J. Phys. Conf. Ser. **136** (2008), doi:10.1088/1742-6596/136/2/022030.
- [51] A. Vaitaitis *et al.*, NuTeV collaboration, Phys. Rev. Lett. **83** (1999) 4943, arXiv:hep-ex/9908011.
- [52] A.M. Cooper-Sarkar *et al.*, WA66 collaboration, Phys. Lett. **B 160** (1985) 207.
- [53] S.R. Mishra *et al.*, CCFR collaboration, Phys. Rev. Lett. **59** (1987) 1397.

- [54] R.E. Shrock, Phys. Lett. **B 96** (1980) 159; R.E. Shrock, Phys. Lett. **B 112** (1982) 382; D.I. Britton *et al.*, Phys. Rev. **D 68** (1992) 3000; D.I. Britton *et al.*, Phys. Rev. **D 46** (1992) 3000; T. Yamazaki *et al.*, Conf. Proc. C840719” (1984) 262; D.A. Bryman and T. Numao, Phys. Rev. **D 53** (1996) 558; R. Abela *et al.*, Phys. Lett. **B 105** (1981) 263; M. Daum *et al.*, Phys. Rev. **D 36** (1987) 2624; R.S. Hayano *et al.*, Phys. Rev. Lett. **49** (1982) 1305; M. Aoki *et al.*, Phys. Rev. **D 84** (2011) 052002.
- [55] A. Atre, T. Han, S. Pascoli and B. Zhang, JHEP **05** (2009) 030, arXiv:hep-ph/0901.3589.
- [56] O. Ruchayskiy and A. Ivashko, JHEP **06** (2012) 100, arXiv:hep-ph/1112.3319.
- [57] F. Bergsma, Ph. D. Thesis, Univ. of Amsterdam, 1990.
- [58] D.E. Groom, M.V. Mokhov S.I. Striganov, Atomic Data and Nuclear Data Tables **78** (2001) 183, doi:10.1006/adnd.2001.0861.
- [59] The LHCb collaboration, CERN/LHCC/2000-007, 17/12/1999.
- [60] NA62 collaboration, NA62-10-07, <http://cds.cern.ch/record/1404985>.
- [61] W. Flegel, private communication 24/8/2013.
- [62] R. Aaij *et al.*, CERN-LHCC-2011-001 (2011).
- [63] J. Dorenbosch *et al.*, CHARM collaboration, Z. Phys. **C 40** (1988) 497.
- [64] T. Sjöstrand and M. Bengtsson, Comp. Phys. Comm. **43** (1987) 367.
- [65] CERN Program Library Long Writeup W5013 (1993).
- [66] C. Andreopoulos *et al.*, Nucl. Instrum. Meth. **A 614** (2010) 87.
- [67] P. Astier, NOMAD collaboration, Nucl. Phys. **B 621** (2002) 3, DOI: 10.1016/S0550-3213(01)00584-3, arXiv:hep-ex/0111057.
- [68] T. Adams *et al.*, arXiv:hep-ex/0905.3004.